PERGAMON

International Journal of Heat and Mass Transfer 44 (2001) 485–497

International Journal of HEAT and MASS TRANSFER

www.elsevier.com/locate/ijhmt

The effect of surfactants on bubble growth, wall thermal patterns and heat transfer in pool boiling

G. Hetsroni[a,*], J.L. Zakin[b], Z. Lin[b], A. Mosyak[a], E.A. Pancallo[b], R. Rozenblit[a]

[a]*Department of Mechanical Engineering, Technion-Israel Institute of Technology, Haifa 32000, Israel*
[b]*Department of Chemical Engineering, Ohio State University, Columbus, OH 42210, USA*

Received 25 October 1999; received in revised form 13 January 2000

Abstract

During nucleate pool boiling of pure water and water with cationic surfactant, the motion of bubbles and the temperature of the heated surface were recorded by a high-speed video camera and an infrared radiometer. All experiments were performed at saturated boiling conditions. The boiling curves for various concentrations were obtained and compared. The results show that the bubble behavior and the heat transfer mechanism for the surfactant solution are quite different from those of pure water. The heat transfer dependence on the relative changes of both the surface tension and the kinematic viscosity was discussed. © 2000 Elsevier Science Ltd. All rights reserved.

Keywords: Boiling; Bubble dynamics; Thermal pattern; Heat transfer

1. Introduction

In boiling heat transfer, it is usually desirable to transfer the largest possible heat flux with the smallest possible temperature difference between the heating surface and the boiling liquid, and to maximize the critical heat flux. Various means have been developed with this aim in mind, including the use of additives to modify the liquid properties. The process of nucleate boiling is the total sum of the processes of bubble initiation, growth and departure. Though these individual processes have been studied much, it is difficult to predict the effect of the physical properties of surface-active agents (surfactants) on the main boiling characteristics, such as the relationship between the heat flux and the temperature difference.

In contrast to the momentum and scalar transfer in turbulent pipe flow with surfactants, which shows a reduction in the friction factor and the heat transfer coefficient [1], the study of surfactant solutions in the pool boiling shows a significant enhancement of the boiling mechanism. The role of surface-active solutes was explored by Morgan et al. [2], for 0.1–1.0% aqueous solutions of a commercial surfactant. They found that the boiling curves (q vs. Δt) were shifted laterally in varying degrees, such that heat transfer was higher than that for pure water, (q is the heat flux, $\Delta t = t_s - t_{sat}$ is the superheat, t_s is the average surface temperature of the heater, t_{sat} is the saturation temperature of the solution). This is an important fact because, if proved

---

* Corresponding author. Tel.: +972-4-829-2058; fax: +972-4-832-4533.

E-mail address: hetsroni@tx.technion.ac.il (G. Hetsroni).

PII: S0017-9310(00)00099-5

Nomenclature

C	the concentration of surfactant
f	the frequency of temperature fluctuations
k	the thermal diffusivity
q	the heat flux
t_s	the average temperature of the heater surface
t_{sat}	the saturation temperature

Greek symbols

Δt	superheat
α	heat transfer coefficient
λ	thermal conductivity
η	shear viscosity
ν	kinematic viscosity
ρ	fluid density
σ	surface tension
ω	shear rate

Subscript

w	pure water

to be applicable under industrial boiling conditions, it may lead to a considerable increase in the power level of all boilers without any increase in size or operating temperature. One interesting field of application of boiling and evaporation is in desalination of seawater, which is becoming essential in some arid regions. It was shown by Sephton [3] in 1974 that addition of small amounts of surfactants to seawater can substantially enhance the boiling process, and reduce the price of the desalinated water to an acceptable level. At that time, the research was discontinued because the environmental impact of surfactants was not known.

Since the concentrations are usually low, addition of the surfactant to water causes no significant change in the saturation temperature and the majority of other physical properties, except for the surface tension and, in some cases, the viscosity. There have been a large number of studies to determine the boiling enhancement mechanism caused by addition of surfactants to water. Frost and Kippenhan [4] investigated boiling of water with varying concentrations of surfactant "Ultra Wet 60L". They found an increase in heat transfer and concluded that it resulted from the reduced surface tension. Heat transfer in nucleate pool boiling of dilute aqueous polymer solutions was measured by Kotchaphakdee and Williams [5] and compared with results for pure water. Photographs showed distinct differences in bubble size and dynamics, between polymeric and non-polymeric liquids. Gannett and Williams [6] concluded that surface tension was not relevant in explaining the enhancement effect, and reported that viscosity could be a generally successful correlating parameter. Nucleate boiling curves for aqueous solutions of drag-reducing polymers have been measured experimentally by Shah and Darby [7] and by Paul and Abdel-Khalik [8]. The explanation of observed changes in the boiling curves was based only on how the polymer additives changed the solution viscosity. Polymer type, concentration and molecular weight were important only insofar as they affect the solution viscosity. Yang and Maa [9] studied pool boiling of dilute surfactant solutions. The surfactants used in this study were sodium lauryl benzene sulfonate and sodium dodecyl sulfate (SDS). Since all experiments were carried out under very low concentrations, it was concluded that these additives had no notable influence over the physical properties of the boiling liquid, except surface tension, which was significantly reduced. This study showed that the surface tension of the boiling liquid had significant influence on the boiling heat transfer coefficient.

Pool boiling experiments were carried out by Tzan and Yang [10], for relatively wide ranges of surfactant concentration and heat fluxes. The results verify again that a small amount of surface-active additive makes the nucleate boiling heat transfer coefficient of water considerably higher. It was also found that there is an optimum additive concentration for highest heat flux. Beyond this optimum point, further increase in the concentration of the additive lowers the boiling heat transfer coefficient. Wu et al. [11] reported experimental data on the effect of surfactants on nucleate boiling heat transfer in water with nine additives. Anionic, cationic, and non-ionic surfactants were studied at concentration up to 400 ppm (parts per million). The enhancement of heat transfer was related to the depression of static surface tension. Boiling heat transfer coefficients were measured by Ammerman and You [12] for an electrically heated platinum wire immersed in saturated water, and in water mixed with three different concentrations of SDS (an anionic surfactant). Their results showed that addition of an anionic surfactant to water caused an increase in the convection component and a corresponding reduction in the latent heat component of the heat flux in the fully developed boiling region. The enhancement of heat transfer at boiling of water, which is caused by the addition of an anionic surfactant, appears to be influenced by this relative change in these heat flux components. The comprehensive reviews on the heat transfer in nucleate pool boiling of aqueous surfactants and polymeric solutions have been published by Kandlikar and Alves [13] and by Wasekar and Manglik [14]. It is shown that surfactant additives at low concentrations can enhance the nucleate boiling heat transfer significantly.

In the present study, we used the cationic surfactant Habon G of molecular weight 500 (trade name Hoe S4089, Hoechst AG) for the boiling enhancement. The cation of the surfactant is hexadecyldimethyl hydroxyethyl ammonium and the counter-ion is 3-hydroxy-2-naphthoate. The surfactant molecules form large rod-shaped micelles. It was shown by Zakin et al. [15] that although microstructure of Habon G was mechanically degraded under high shear conditions, it recovered quickly — no matter how many times it was broken up by shear.

The objective of the present study is to determine how the nucleate boiling is affected by the addition of Habon G to water, and to generalize the data on the heat transfer enhancement for a wide range of concentration of surfactants.

Saturated pool boiling on a heated surface and on a heated tube was studied and the effect of the surface tension and viscosity on the heat transfer coefficient has been examined.

2. Physical properties of solutions

The measurements of physical properties were carried out over a wide range of temperatures and for various concentrations. All the solutions used were prepared by dissolving the powdered surfactant in deionized water, with gentle stirring, over a period of several days. Concentrations investigated here were 65–1060 ppm. Typical results are presented and discussed below.

The shear viscosity of all surfactant solutions was determined in the temperature range 25–60°C with Rheometrics Fluids Spectrometer RFS II using a Couette system. The standard deviation is 4%. Fig. 1 shows the effect of shear rate ω on shear viscosity η for a 530 ppm Habon mixture, at different temperatures. The curves come closer to one another for higher shear rate values. The magnitude of the shear viscosity as a function of the shear rate decreases, when the temperature of the solution increases. Moreover, the shear viscosity η does not change significantly in the range of the shear rate $\omega = 1\text{–}1000\ \mathrm{s}^{-1}$ at $t = 60°\mathrm{C}$. Based on this result, we studied the viscosity behavior of Habon G solution after boiling, using a Cannon–Fenske capillary viscometer, at high shear rates for temperatures of 55°C and above.

Fig. 2 shows the effect of temperature on the kinematic viscosity of the surfactant solution at various Habon G concentrations. One can see here the similar tendency of viscosity curve to approach that of pure water near the saturation temperature. Such behavior is more pronounced as the solution concentration decreases.

We also measured the thermal conductivity of Habon G solution. The apparatus was of the steady-state type. Both the clear water and the tested surfactant solution were enclosed in two identical cells. The top of each cell was made of 50 μm stainless steel foil, heated by DC current and the bottom was cooled by water. The difference between inlet and outlet water temperature did not exceed 0.2°C. The thermal field of the cell top was measured by infrared (IR) radiometer. During these measurements, the thermal pattern associated with free convection was not observed. Fig. 3 shows the dependence of thermal conductivity λ on the

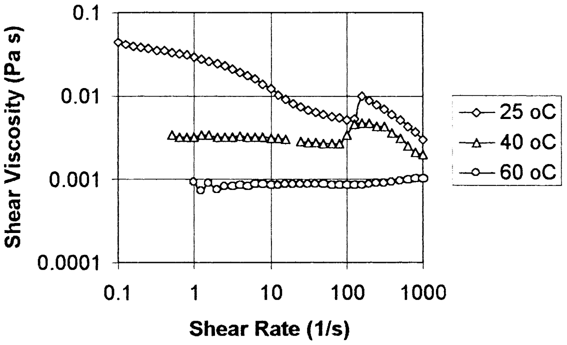

Fig. 1. The shear viscosity of 530 ppm Habon G solution versus shear rate.

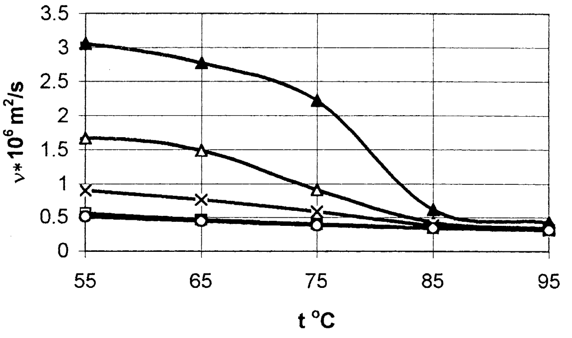

Fig. 2. Kinematic viscosity of solution versus temperature at various Habon G concentration. ○ — water; Habon G: □ — 130 ppm, × — 260 ppm, △ — 530 ppm, ▲ — 1060 ppm.

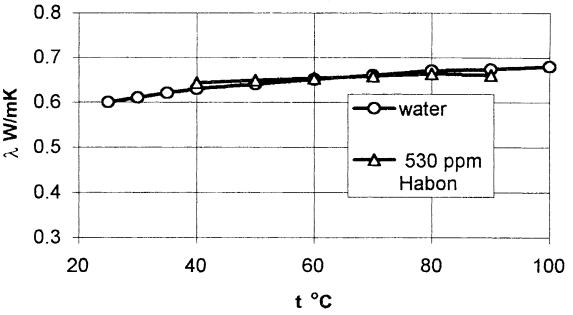

Fig. 3. Thermal conductivity versus temperature.

temperature t for the 530 ppm Habon G solution. The value of the thermal conductivity agrees well with that for pure water within the uncertainty of the measurements. The standard deviation of the thermal conductivity measurements is 2%.

The surface tension was measured in the temperature range of 25–70°C with standard deviation of 2%. The data were obtained using a SensaDyne PC500-LV Surface Tensiometer System, which measures surface tension within the body of a test fluid by blowing a bubble of gas through two probes of different diameters inside the body.

Fig. 4 shows the magnitude of surface tension as a function of the temperature for various concentrations of Habon G. As seen in this figure, the surface tension decreases with increase in both concentration and temperature. The temperature effect on the surface tension is much stronger at temperatures near the saturation temperature, whereas the opposite trend is observed for the viscosity. The physical properties of the solutions used in the present study are given in Table 1.

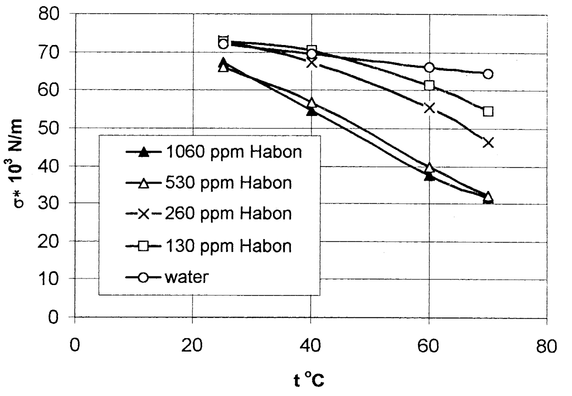

Fig. 4. The surface tension as a function of temperature at various Habon G concentrations.

3. Experimental

3.1. Apparatus

Two sets of apparatus were used. Fig. 5a shows the one designed for the study of pool boiling from a horizontal heating surface facing upward. Boiling occurred over a constantan foil, 50 μm thick, attached to the window at the bottom of the vessel. The foil was heated by DC current and the heat flux on the wall could be regulated and measured. The IR image of the heater was recorded from below by an IR radiometer. Heat losses were reduced by proper insulation and did not exceed 1%. Boiling on the heated foil was illuminated and photographed through view windows on the sides of the apparatus.

The second apparatus, as shown in Fig. 5b was designed for the studies of the heat flux $q > 100$ kW m^{-2}. The construction of this apparatus was similar to the one described above except that the heating element was made of a stainless steel tube with an outer

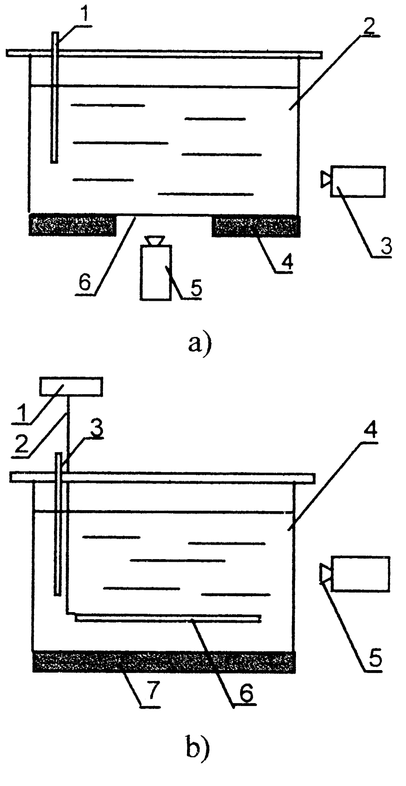

Fig. 5. (a) Apparatus for pool boiling on a horizontal surface. 1: supplementary heater, 2: window, 3: high speed video camera, 4: insulation, 5: IR camera, 6: heated foil. (b) Apparatus for pool boiling on a tube. 1: temperature measurements, 2: thermocouple, 3: supplementary heater, 4: window, 5: high-speed camera, 6: heating tube, 7: insulation.

diameter of 1.5 mm. The electric current was supplied to this heating element through two copper bars and DC power supply. A calibrated Teflon coated T-type thermocouple was inserted inside of the tubular heating element. The joint of the thermocouple could be adjusted exactly to any desired position in the heating element. The temperature of the outer surface was calculated from the power generation per unit volume of the electrically heated tube. The measurements showed that the temperature along the tube was uniform, with an accuracy of ±0.1°C.

3.2. Instrumentation

The growth of bubbles and the bubble motion near the heated surface were recorded by a high-speed video camera with recording rate up to 10,000 frames s^{-1}. The playback speed can be varied from a single frame to 250 frames s^{-1}.

An IR radiometer was used in the investigation of thermal patterns. The radiometer has a typical minimum detectable temperature difference of 0.1 K. Time response of this instrument is limited by the video system format (25 frames s^{-1}). The image has horizontal resolution of 256 pixels per line and 256 intensity levels. Since the foil was very thin, the temperature difference between the two sides of the foil did not exceed 0.2 K at a heat flux of 100 kW m^{-2}. Therefore, the time-averaged temperature was almost the same on both sides of the foil. The radiometer allows to obtain a quantitative thermal profile in the line mode, the average temperature in the area mode, and the temperature of a given point in the point mode. We had to consider the frequency response of the system to changes in the heat transfer coefficient. It was shown by Hetsroni and Rozenblit [16] that temperature distortions and phase shift in temperature fluctuations on the heated wall begin at $f = 15$–$20\ s^{-1}$. In the present study, the highest frequency of the bubble departure was higher, so we confined our measurements to average temperature and qualitative observation of the thermal structure on the heated bottom. The surface temperature and the surfactant mixture temperature were measured with an accuracy of ±0.1°C. Electrical power was determined by means of a digital wattmeter with an accuracy of ±0.5%.

3.3. Procedure

The heating surface was cleaned routinely before and after each set of three data points with a sequence of operations involving application of constantan cleaner and washing with hot tap water and deionized water. Only a soft sponge and absorbent paper tissues contacted the constantan, which remained smooth and completely wettable.

During a typical run, the boiler was loaded with 1500 ml of liquid to bring the surface to a level 70–80 mm above the heater. Steady state boiling was achieved in 10–20 min after the supplementary heater was turned on, this was determined by monitoring the temperature of the solution. Surfactant solutions were replaced with fresh samples after three runs. This precaution was taken in order to minimize changes in solution properties, which might have occurred at high temperature due to evaporation over long periods of time.

These occasions of sample renewal permitted regular observations of the heater surface. No visible deposits formed under test conditions, based on observations in the test runs and after draining the boiler. Room temperature was maintained at 23°C, so that heat losses from the boiler would be nearly constant in all runs.

4. Boiling behavior

4.1. Bubble visualization

The evolution of vapor bubbles in a boiling liquid, in particular the growth of bubbles, is one of the parameters determining the intensity of the heat transfer

Table 1
Physical properties of the solutions

Concentration (ppm)	Surface tension $\sigma * 10^3$ (N m^{-1})				Kinematic viscosity $\nu * 10^6$ ($m^2\ s^{-1}$)		
	Temperature (°C)				Temperature (°C)		
	25	40	60	70	55	75	95
0	71.95	69.65	66.22	64.35	0.51	0.38	0.31
130	72.85	70.55	61.25	54.7	0.56	0.40	0.31
260	72.95	67.4	55.5	46.55	0.90	0.58	0.31
530	65.95	56.9	39.8	32.3	1.67	0.91	0.34
1060	67.3	54.75	37.5	31.55	3.05	2.22	0.43

from a heated surface. The growth of the bubble in the liquid containing surfactants is affected by a number of specific factors.

The pool boiling experiments were carried out under atmospheric pressure. The phenomenon of foaming, often observed during boiling in the presence of surfactant, was also found for all Habon G solutions. The foam formed on the surface of the solution and its height increased with the heat flux. In the present study, the height of the liquid phase over the heater was no less than 60 mm throughout all experiments. The bubble behavior was recorded at 1000 frames s^{-1}

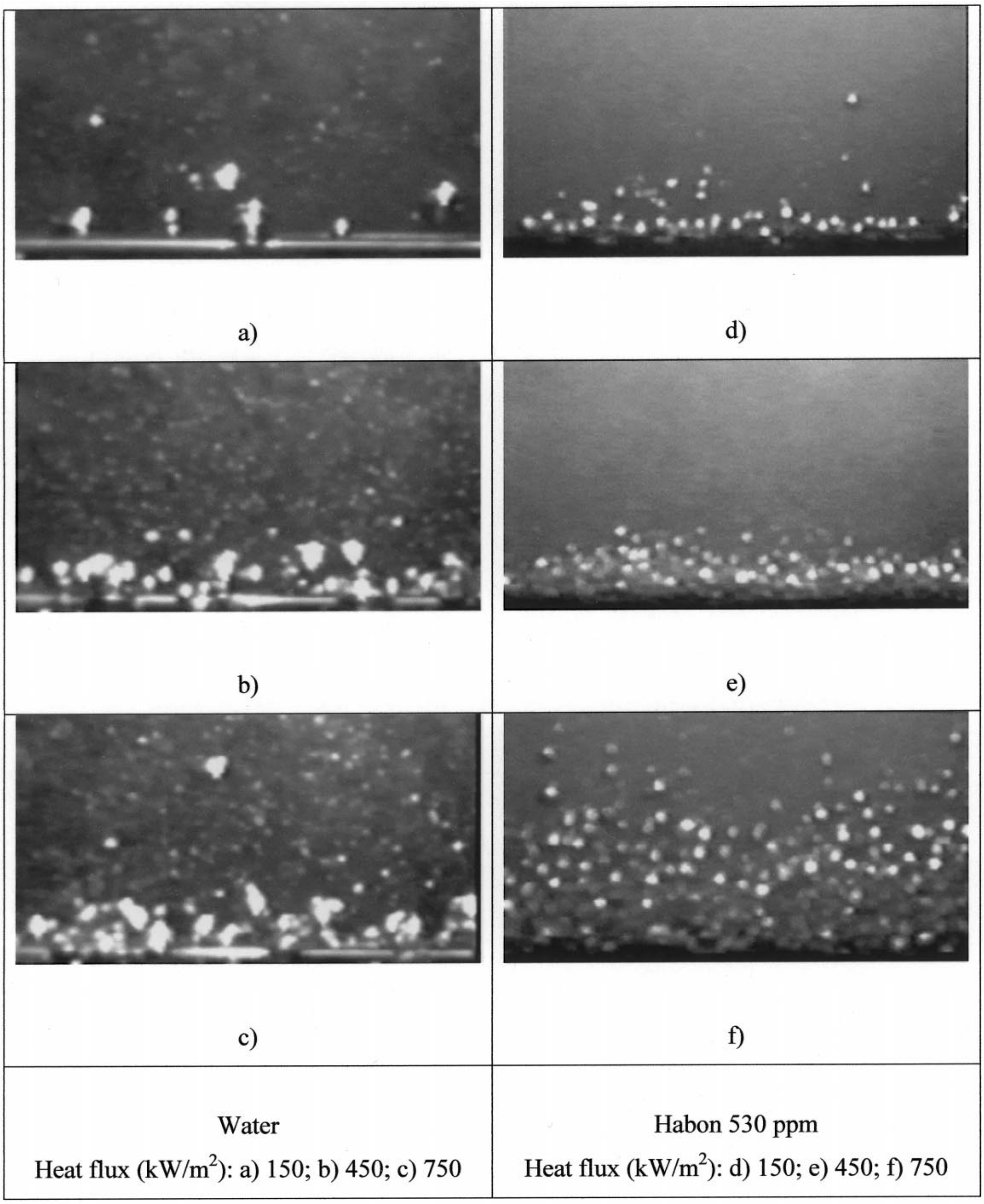

Fig. 6. Boiling of water (a–c) and 530 ppm Habon G solution (d–f) on the pipe at various heat fluxes.

by the high-speed camera. The typical stages of bubble growth analyzed for this study are shown in Figs. 6 and 7. The field of view is 40 × 30 mm in the horizontal and vertical directions, respectively.

Fig. 6a–c show typical pictures for water boiling on the pipe of 1.5 mm outer diameter at heat fluxes $q = 150$, 450, 750 kW m^{-2}, respectively. A population of bubbles was observed in the vicinity of the heated tube. The bubble dynamics for water are seen to depend on heat flux, similar to well-known boiling visualization data. After the onset of nucleate boiling, the regime of single bubbles occurs close to the heated wall (Fig. 6a). As the heat flux increases, bubble coalescence takes place (Fig. 6b). This phenomenon is

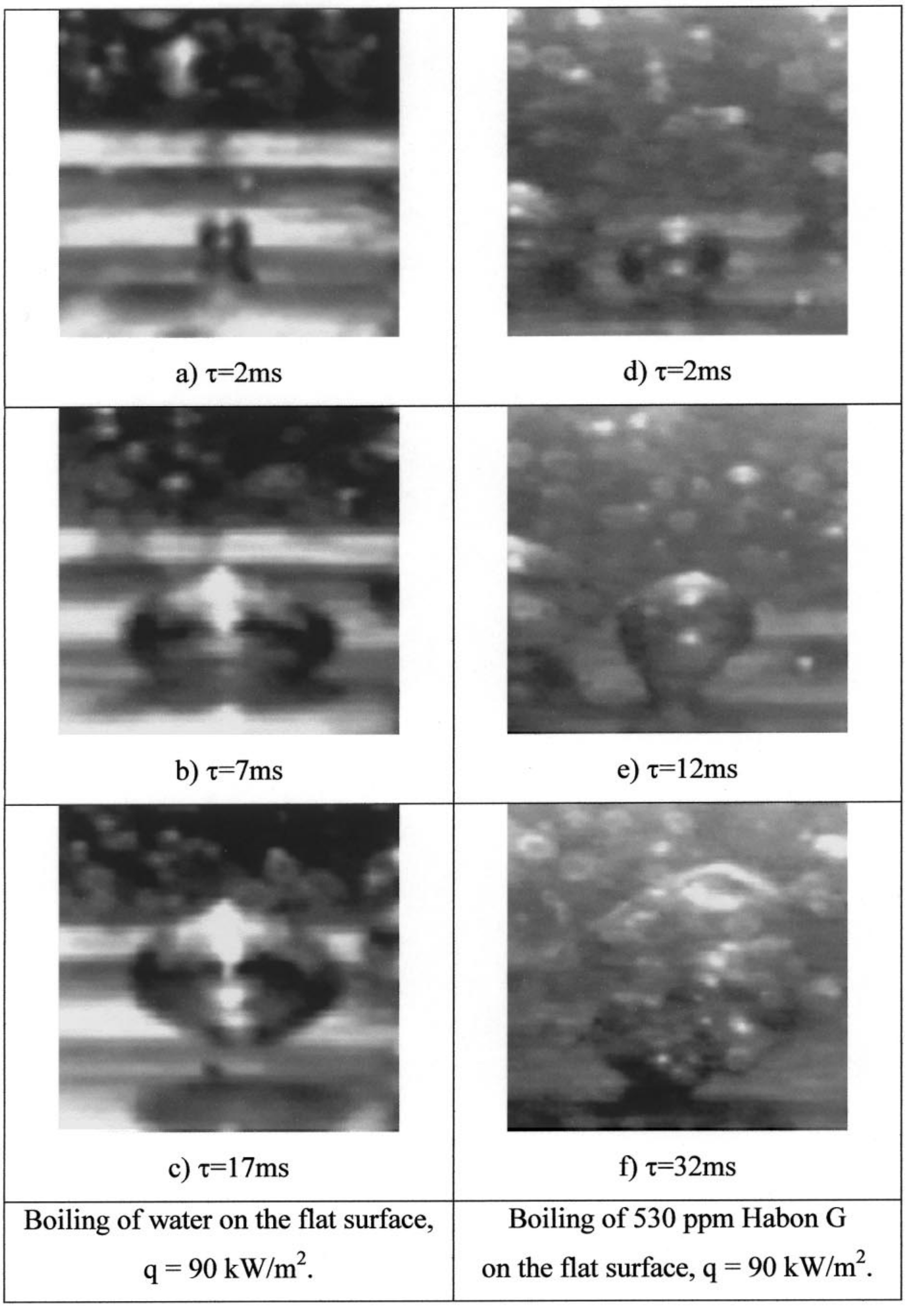

a) τ=2ms

b) τ=7ms

c) τ=17ms

Boiling of water on the flat surface, q = 90 kW/m^2.

d) τ=2ms

e) τ=12ms

f) τ=32ms

Boiling of 530 ppm Habon G on the flat surface, q = 90 kW/m^2.

Fig. 7. The dynamics of bubble growth on the heated flat plate in clear water and 530 ppm Habon G solution.

more pronounced at $q = 750$ kW m^{-2} (Fig. 6c). For pure water, the average bubble size was observed to slightly increase with increasing heat flux. The bubbles have an irregular shape at all values of heat flux. Fig. 6d–f show boiling of the 530 ppm Habon G solution under the same conditions. The Habon G additive reduces significantly the tendency of coalescence between vapor bubbles. Here, too, there is a weak tendency toward increasing the average diameter as heat flux increases. In this case, the shape of bubbles is closer to spherical than for pure water.

To study the bubble dynamics and the thermal pattern on a horizontal surface, the experimental setup, shown in Fig. 5a, was used. The process of single bubble growth, at heat flux $q = 90$ kW m^{-2}, is presented in Fig. 7a–f for water and Habon G solution. Fig. 7a–c show the bubble initiation, the bubble growth after 7 ms and the bubble departure after 17 ms for water pool boiling. In the case of boiling 530 ppm Habon G solutions (Fig. 7d–f), the time from the bubble initiation to its departure is about twice as long as that for pure water. For Habon G solutions boiling on the horizontal heating surface facing upward, we sometimes observed the formation of a large number of secondary bubbles (Fig. 7f) at the departure time of the initial bubble.

The effect of surfactant additive on boiling may also be attributed to the departure from equilibrium surface tension which is produced by rapid extension of the vapor liquid interface during growth and coalescence of the vapor bubbles in the vicinity of the boiling surface. Wu et al. [17] have investigated this effect. They tried to correlate the nucleate boiling heat transfer coefficient with the equilibrium and dynamic surface tension of the aqueous surfactant solutions. Their results revealed that neither equilibrium nor dynamic surface tension could successfully explain boiling phenomena. On the other hand, different behavior of bubbles above the heater surface and non-monotonous behavior of boiling curves with increasing heat flux suggest that different heat transfer mechanism may prevail in surfactant solutions. Boiling with surfactant additives is generally a very complex process and it is influenced by a larger set of variables in comparison to the phase-change process of pure water. Besides the surface tension, the nucleate boiling behavior is also dependent on, among others, heat flux, thermal patterns on the heated surface, Marangoni effects and critical micelle concentration (c.m.c.) of the surfactant. These issues are discussed in this paper and some new data for the saturated pool boiling of surfactant solutions are also presented.

4.2. Visualization of thermal pattern on the heated wall

Although IR thermography applied to boiling has relatively low frequency response, it is still more accurate than surface temperature measurement by micro thermocouples or resistance thermometers. Its advantages are the extensive nature of the measurements and the absence of disturbance to the microgeometry of the boiling surface.

The examples given in this paper are just a small sample of the information contained in the recordings. They illustrate the advantages and limitations of IR thermography combined with video recording for the study of boiling heat transfer. The technique is necessarily limited to boiling on very thin walls, conditions that maximize the local variations in wall temperature and minimize lateral conduction.

The spatial distributions (Fig. 8) show variations of wall temperature of about 17 K for water (Fig. 8a) and 25 K for surfactant (Fig. 8b). With such wide ranges, it is clear that models for the bubble nucleation and growth that assume uniformity of wall superheat cannot be realistic. The IR thermography samples and the histograms of the thermal fields show that instantaneous values of the surface temperature, t_s, are lower for the Habon G solutions. This means that the average heat transfer coefficient in the surfactant solution increases as compared to boiling of water. Moreover, the larger width of the histogram for Habon G solution means that higher values of local heat transfer caused more intensive vaporization, which could happen more often than with boiling of water.

4.3. Boiling curves and heat transfer coefficients

In Fig. 9, experimental boiling heat transfer data are presented as a function of heat flux versus heater superheat (space–time average values at the fluid–solid interface). As the heat flux increases, the boiling curve shifts towards left as the concentration of Habon G increases.

It can be seen that the boiling curve at concentration of 1060 ppm is close to the curve for 530 ppm Habon G solution, and at high values of heat flux shifts towards right. Thus, it is evident that the influence of the surfactant on the boiling curve behavior has an optimum, depending on the concentration. For each concentration, 12 runs were performed: six runs for increasing heat flux and the remaining six for decreasing heat flux. Each point in Figs. 9 and 10 represents an average value obtained from these measurements. We did not observe any signs of hysteresis. The onset of nucleate boiling point (in terms of a mean boiling excess temperature) is not affected by the surfactant concentration.

The effect of heat flux and additive concentration on the nucleate boiling heat transfer coefficient of Habon G solutions is more evident if the experimental data are expressed as a plot of heat transfer coefficient versus heat flux, as shown in Fig. 10. The heat transfer coefficient increases as the heat flux and concentration are increased, except when the heat flux level is higher than about $q = 300$ kW m^{-2} and the concentration is higher than 530 ppm. Of these two trends, the former is consistent with results observed previously [7,9,10]. The maximum in heat transfer coefficient at a certain concentration has seldom been reported. This may be attributed to the fact that the solutions tested were usually too dilute and/or the heat flux level was too low in most of the past experiments reported in the literature. Our data of heat transfer for 1060 ppm Habon G solution agree qualitatively with boiling heat transfer results reported by Tzan and Yang [10]. They demonstrated that the effect of surfactant additives on nucleate boiling heat transfer decreases, when the concentration of SDS solution was higher than 700 ppm.

5. The effect of physical properties of surfactant solution on heat transfer

A detailed investigation of the physical characteristics of the surfactant can demonstrate the effect of

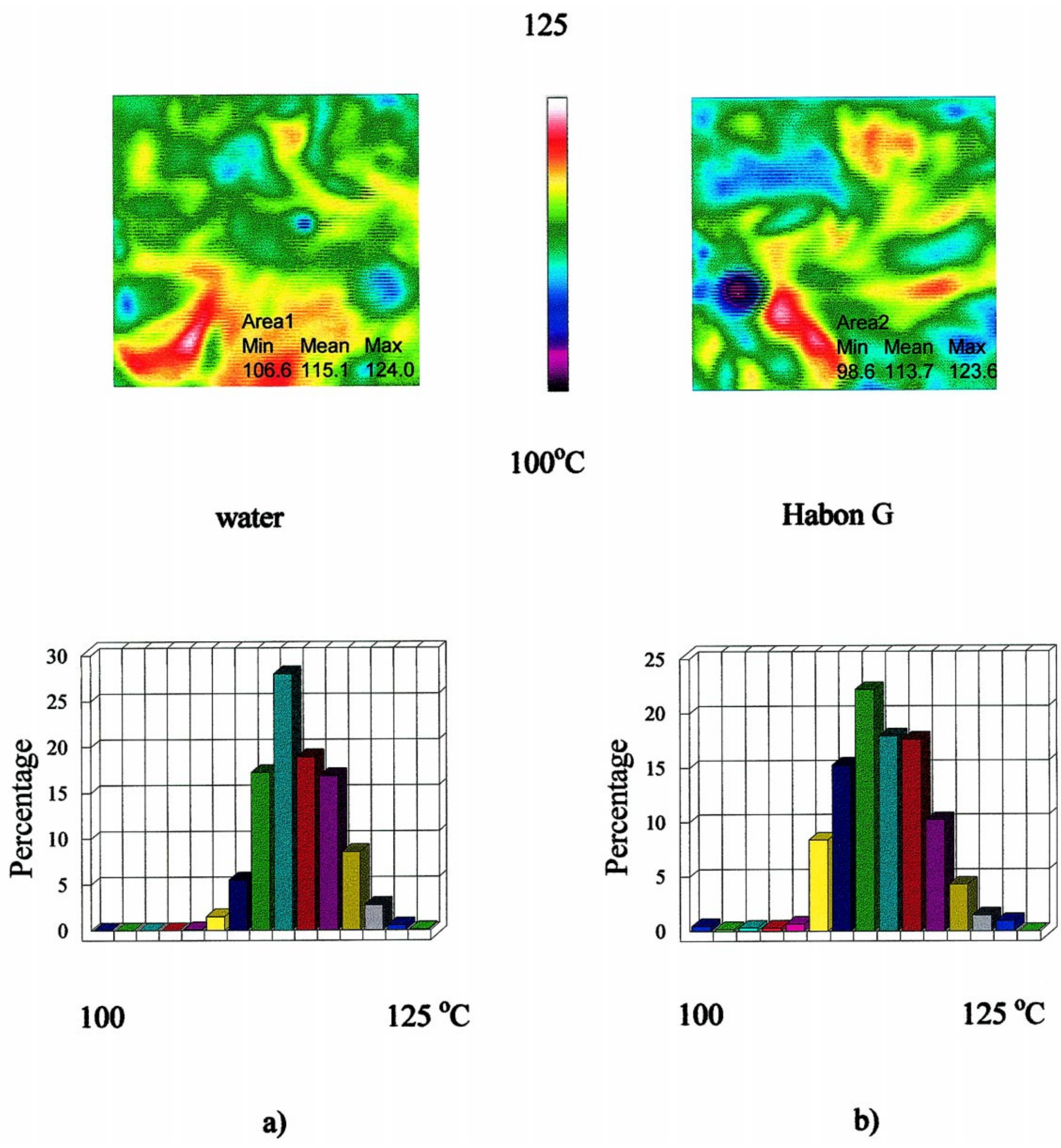

Fig. 8. Thermal patterns and histograms of the temperature at pool boiling of water (a) and Habon G solution (b) on the flat plate ($q = 90$ kW m^{-2}).

different properties of the mixture on the heat transfer. Fig. 11 shows the dependencies of the relative surface tension σ/σ_w and the relative viscosity ν/ν_w as a function of Habon G concentration, where σ and σ_w are the surface tensions, ν and ν_w are the kinematic viscosities for the Habon G solution and pure water, respectively. One can see that the magnitude of relative surface tension decreases gradually from 1.0 for pure water to about 0.5 at 530 ppm surfactant solution. Further increase in the surfactant concentration does not significantly affect the value of the surface tension. On the other hand, the value of the kinematic viscosity (the right axis in Fig. 11) is practically equal to that of pure water at low surfactant concentrations (<300 ppm of Habon G), while further increase in additive concentration leads to significant increase in viscosity. Such complicated behavior of physical properties inevitably affects the complex behavior of the heat transfer coefficient in boiling.

To clarify the effect of concentration on heat transfer, we compared our results with the data of investigations on heat transfer enhancement, where maximum heat transfer enhancement has also been reached at a certain concentration of surfactant solution. The comparison is shown in Fig. 12 as the enhancement of the heat transfer coefficient $\alpha/\alpha_w - 1$ versus concentration of different surfactant solutions (where α and α_w are the heat transfer coefficients in the surfactant solution and pure water, respectively; SDS is the anionic surfactant "sodium dodecyl sulfate"). These curves have different values of heat transfer enhancement depending on the kind of surfactant and the heat flux. However, they have similar trends with increasing surfactant concentration. Heat transfer increases at low surfactant concentration, reaches a maximum and further increase in the amount of additive leads to a decrease in the heat transfer coefficient. The value of this maximum depends on the heat flux (for example points A_1 and A_2 for Habon G solution and on the kind of surfactant (points B_1, B_2 for SDS [11]).

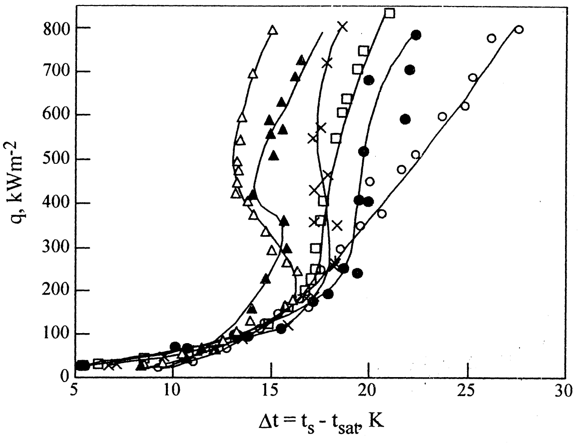

Fig. 9. Boiling curves of water and aqueous Habon G solutions: ○ —water; Habon G: ● — 65 ppm, □ — 130ppm, × — 260 ppm, △ — 530 ppm, ▲ — 1060 ppm.

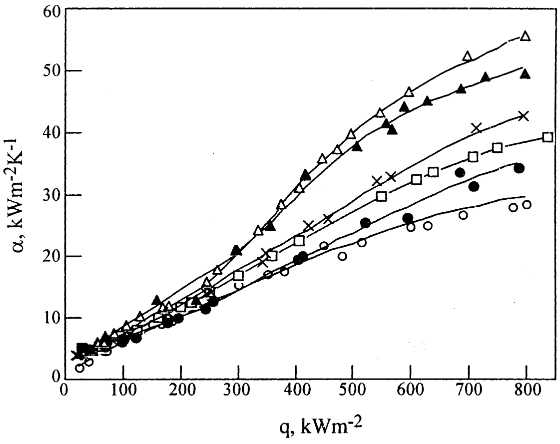

Fig. 10. Boiling heat transfer coefficient (symbols as in Fig. 9).

The curves for a given kind of surfactant reach their maximum at some definite value of surfactant concentration. Such a behavior may be explained by the effect of changing surface tension with surfactant concentration. In Fig. 13, the dependencies of the surface tension for the various surfactants discussed are shown. We can see that beginning from some particular value of surfactant concentration (which depends on the kind of surfactant), the value of the relative surface tension almost does not change with further increase in the surfactant concentration. Such a behavior agrees with results presented by Wasekar and Manglik [14] and may be referred to the c.m.c. of the surfactant. In

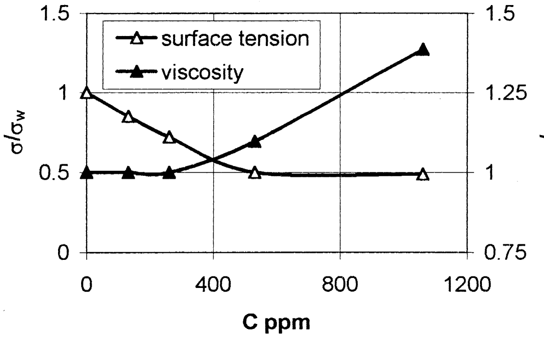

Fig. 11. The relative surface tension σ (at $t = 70°C$) and kinematic viscosity ν (at $t = 95°C$) as a function of Habon G concentration.

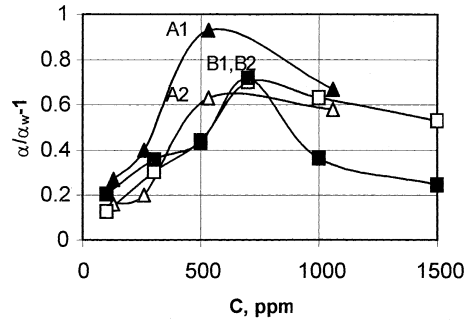

Fig. 12. The heat transfer enhancement for various surfactant solutions at different heat fluxes as a function of surfactant concentration (Habon G: △ — q = 400 kW m^{-2}; ▲ —q = 800 kW m^{-2}; SDS [10]: □ — q = 350 kW m^{-2}; ■ — q = 400 kW m^{-2}).

Fig. 13, the data for Habon G are presented at the temperature $t = 70$°C, the data for SDS are reported at the temperature 25°C [10,11], and at $t = 100$°C [17]. Unfortunately, the data [17] are measured up to $C =$ 400 ppm only. However, it should be emphasized that the variation of the non-dimensional surface tension as a function of the surfactant concentration shows the same behavior for various temperatures. The normalized nucleate boiling heat transfer coefficient may be related to normalized surface tension of the surfactant solution. We used the magnitude of surfactant concentration where the change of relative surface tension reaches 90% of the complete change to normalize the concentration scale. The values C_0 = 530 and 700 ppm were chosen for Habon G and SDS solutions, respectively.

For normalization of the value of the heat transfer enhancement, we used its magnitude at the maximum for each curve. The result of such normalization is shown in Fig. 14. In this figure, C is the solution concentration, C_0 is the characteristical concentration, α is the heat transfer coefficient at given values of the solution concentration and the heat flux q, $\alpha_{\max}$ is the maximum value of the heat transfer coefficient at the same heat flux, α_w is the heat transfer coefficient for pure water at the same heat flux q. Data from all the sources discussed reach the same value of 1.0 at the magnitude of relative surfactant concentration equal to 1.0.

Thus, the enhancement of heat transfer may be connected to the decrease in the surface tension value at low surfactant concentration. In such system of coordinates, the effect of the surface tension on excess heat transfer $(\alpha - \alpha_w)/(\alpha_{\max} - \alpha_w)$ may be presented as linear fit of the value C/C_0. On the other hand, the decrease in heat transfer at higher surfactant concentration may be related to the increased viscosity. Unfortunately, we did not find surfactant viscosity data in the other studies. However, we can assume that the effect of viscosity on heat transfer at surfactant boiling becomes negligible at low concentration of surfactant only.

The surface tension of a rapidly extending interface in surfactant solution may be different from the static value, because the surfactant component cannot diffuse to the absorber layer promptly. This may result in an interfacial flow driven by the surface tension gradient $\Delta\sigma$ (known as Marangoni flow).

We consider a fluid zone of thickness d across which the surface tension difference is $\Delta\sigma$. The Marangoni number $Ma = \Delta\sigma \cdot d/\rho\nu k$ is the controlling parameter of this type of flow that affects the heat transfer coefficient. As it is seen in Fig. 11, the surface tension decreases significantly, whereas the kinematic viscosity

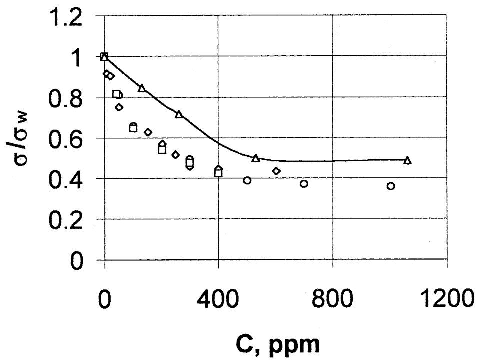

Fig. 13. The non-dimensional surface tension of various surfactants versus solution concentration (◇ —SDS [11], t = 25°C; ○ — SDS [10], t = 25°C; □ — SDS [18], t = 100°C; △ — Habon G [present study], t = 70°C).

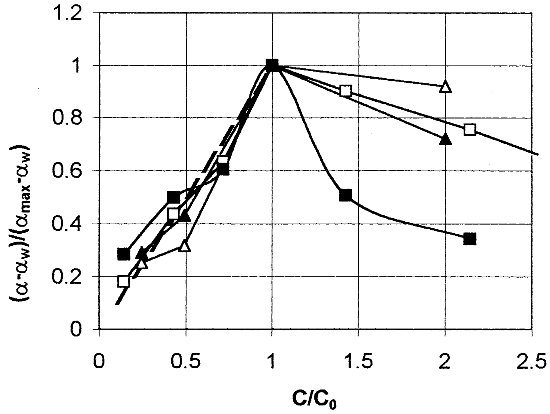

Fig. 14. The excess heat transfer coefficient versus the surfactant concentration (Habon G: △ — q = 400 kW m^{-2}; ▲ — q = 800 kW m^{-2}; SDS [10]: □ — q = 350 kW m^{-2}; ■ — q = 400 kW m^{-2}).

almost does not change with concentration increase at low solution concentration. The Marangoni number can be expressed as $Ma = Re \cdot Pr$, where $Re = \Delta\sigma \cdot d/\rho\nu^2$ and $Pr = \nu/k = \nu c\rho/\lambda$ are the Reynolds number and Prandtl number, respectively. The density ρ, specific heat c and thermal conductivity λ (Fig. 3) of Habon G solution are the same as for water. Thus, the Reynolds number increases whereas the Prandtl number almost does not change, at low surfactant concentration. Such a behavior of dimensionless parameters explains the increase in the heat transfer coefficient at low concentration of surfactant solution. On the other hand, the Reynolds number decreases proportional by to ν^2, whereas the Prandtl number increases proportional by to the kinematic viscosity ν at higher solution concentration. Fig. 11 shows that the surface tension almost does not change. In this case, the Marangoni effect acts in the opposite direction and suppresses the boiling heat transfer.

6. Conclusions

The experimental results are summarized as follows:

6.1. The difference in boiling behavior

The addition of small amount of cationic surfactant Habon G makes the boiling behavior quite different from that of pure water. For water, bubble action is seen to be extremely chaotic, with extensive coalescence during the rise. Bubbles formed in Habon G solutions were very much smaller than those in water and the surface became covered with them faster. It is known that reduced surface tension results in a decrease of energy required to create a bubble and thus in more bubbles and smaller ones. The boiling excess temperature becomes smaller and the vapor bubbles are formed more easily.

6.2. Thermal pattern on the heated surface

Pool boiling of both water and Habon G solutions on a thin, electrically heated constantan plate in a pool was investigated by IR thermography in combination with video recording. The experiments show that the limitations of the IR technique with respect to frequency response are outweighed by its unique capacity to measure wall temperature distribution with high spatial resolution over an area encompassing many nucleation sites and over long periods. The measurements confirm the importance of the magnitude of wall temperature fluctuations for the removal of heat by bubbles. The histograms of the thermal fields of the heated wall show the decrease in the average temperature and increase in the magnitude of standard deviation for surfactant solutions as compared with water. It means that the heat transfer coefficient in the surfactant solution increases and vaporization is more intensive, compared to water boiling.

6.3. Effect of surfactant solution properties on heat transfer

The boiling curves of surfactant are quite different from the boiling curve of pure water. Experimental results demonstrate that the heat transfer coefficient of the boiling process can be enhanced considerably by the addition of a small amount of Habon G. The heat transfer increases at low surfactant concentration reaches a maximum and decreases with further increase in concentration. The effect of both the surface tension and the kinematic viscosity of surfactant mixture can explain the features of heat transfer at boiling of surfactant solutions.

The decrease in the magnitude of the relative surface tension from 1.0 for pure water to value of about 0.5 for 530 ppm surfactant solution is accompanied by heat transfer enhancement. Further increase in the surfactant concentration does not result in a significant change in the value of the surface tension. On the other hand, the value of relative kinematic viscosity is practically equal to 1 at low surfactant concentrations (<300 ppm of Habon G). Further increase in additive concentration leads to an increase in the viscosity. It is accompanied by a decrease in the heat transfer coefficient. Thus, the enhancement of heat transfer is connected to the decrease in surface tension values at low surfactant concentration, whereas the decrease in heat transfer at higher surfactant concentrations is related to the increase in viscous characteristics.

Acknowledgements

This research was supported by the Fund for the Promotion of Research at the Technion. A. Mosyak and R. Rozenblit are supported by The Ministry of Absorption, State of Israel. This research was also supported by the Israeli Ministry of Science.

References

[1] G. Hetsroni, J.L. Zakin, A. Mosyak, Low-speed streaks in drag reduced turbulent flow, Phys. Fluids 9 (1997) 2397–2404.

[2] A.I. Morgan, L.A. Bromley, C.R. Wilke, Effect of surface tension on heat transfer in boiling, Ind. Eng. Chem. 41 (1949) 2767–2771.

[3] H. Sephton, US Patent No. 3846254, 1974.

[4] W. Frost, C.J. Kippenhan, Bubble growth and heat

transfer mechanisms in the forced convection boiling of water containing a surface active agent, Int. J. Heat Mass Transfer 10 (1967) 931–949.

[5] P. Kotchaphakdee, M.C. Williams, Enhancement of nucleate pool boiling with polymeric additives, Int. J. Heat Mass Transfer 13 (1970) 835–848.

[6] H.J. Gannet Jr., M.C. Williams, Pool boiling in dilute non-aqueous polymer solutions, Int. J. Heat Mass Transfer 14 (1971) 1001–1005.

[7] B.H. Shah, R. Darby, The effect of surfactant on evaporative heat transfer in vertical film flow, Int. J. Heat Mass Transfer 16 (1973) 1889–1903.

[8] D.D. Paul, S.I. Abdel-Khalik, Nucleate boiling in drag-reducing polymer solutions, Journal of Rheology 27 (1983) 59–76.

[9] Y.M. Yang, J.R. Maa, Pool boiling of dilute surfactant solutions, Journal of Heat Transfer 105 (1983) 190–192.

[10] Y.L. Tzanand, Y.M. Yang, Experimental study of surfactant effects on pool boiling heat transfer, Journal of Heat Transfer 112 (1990) 207–212.

[11] W.T. Wu, Y.M. Yang, J.R. Maa, Enhancement of nucleate boiling heat transfer and depression of surface tension by surfactant additives, Journal of Heat Transfer 117 (1995) 526–529.

[12] C.N. Ammerman, S.M. You, Determination of the boiling enhancement mechanism caused by surfactant addition to water, Journal of Heat Transfer 118 (1996) 429–435.

[13] S.G. Kandlikar, L. Alves, Effects of surface tension and binary diffusion on pool boiling of dilute solutions: an experimental assessment, Journal of Heat Transfer 121 (1999) 488–493.

[14] V.M. Wasekar, R.M. Manglik, A review of enhanced heat transfer in nucleate pool boiling of aqueous surfactant and polymeric solutions, Enhanced Heat Transfer 6 (1999) 135–150.

[15] J.L. Zakin, J. Myska, Z. Chara, New limiting drag reduction and velocity profile asymptotes for nonpolymeric additives systems, AIChE Journal 42 (1996) 3544–3546.

[16] G. Hetsroni, R. Rozenblit, Heat transfer to a liquid–solid mixture in a flume, Int. J. Multiphase Flow 20 (1994) 671–689.

[17] W.T. Wu, Y.M. Yang, J.R. Maa, Nucleate pool boiling enhancement by means of surfactant additives, Experimental Thermal and Fluid Science 18 (1998) 195–209.

[18] W.T. Wu, Y.M. Yang, Enhanced boiling heat transfer by surfactant additives, in: Pool and External Flow Boiling, ASME, New York, 1992, pp. 361–366.